DOI: 10.1534/genetics.107.078360

A Mosaic Genetic Screen for Drosophila Neoplastic Tumor Suppressor Genes Based on Defective Pupation

Laurent Menut, Thomas Vaccari, Heather Dionne, Joseph Hill, Geena Wu and David Bilder[1]

Department of Molecular and Cell Biology, University of California, Berkeley, California 94720

Manuscript received July 3, 2007
Accepted for publication August 31, 2007

ABSTRACT

The Drosophila neoplastic tumor suppressor genes (TSGs) coordinately control cell polarity and proliferation in epithelial and neuronal tissues. While a small group of neoplastic TSG mutations have been isolated and their corresponding genes cloned, the regulatory pathways that normally prevent inappropriate growth remain unclear. Identification of additional neoplastic TSGs may provide insight into this question. We report here the design of an efficient screen for isolating neoplastic TSG mutations utilizing genetically mosaic larvae. This screen is based on a defective pupation phenotype seen when a single pair of imaginal discs is homozygous for a neoplastic TSG mutation, which suggests that continuously proliferating cells can interfere with metamorphosis. Execution of this screen on two chromosome arms led to the identification of mutations in at least seven new neoplastic TSGs. The isolation of additional loci that affect hyperplastic as well as neoplastic growth indicates the utility of this screening strategy for studying epithelial growth control.

THE imaginal discs of the Drosophila larva have long served as a model system in which to understand the control of organ size. Imaginal discs are epithelial sacs that, following metamorphosis, will form much of the adult tissue. The primordia of these discs are set aside in the embryo as small groups of 20–50 cells that remain diploid while much of the rest of the animal becomes polyploid. Over the 4 days that span the three larval instars, these primordia proliferate by ~1000-fold to approach their final size. The size of the imaginal disc at the initiation of pupation is a major determinant of the size of the adult organ following metamorphosis. This size is highly regular, reflecting the importance for appropriate physiology and functioning of, for example, the complex optics of the compound eye or the aerodynamics of the wing and haltere flight organs. Thus, tight developmental controls must exist to permit sufficient but not excessive growth of the imaginal discs.

Classic and contemporary manipulative studies have been performed to define the general parameters controlling growth of discs. These studies indicate that growth control is largely intrinsic to the disc (Bryant and Simpson 1984). While the bulk of imaginal disc growth takes place in the larvae prior to pupation, transplanted discs can proliferate in other growth-permissive environments, such as adult abdomens. In this context, discs cease proliferation at approximately the appropriate final size, indicating that the mechanisms that terminate growth are disc autonomous and do not require specific systemic or hormonal cues such as those associated with metamorphosis. Consistent with this, artificially extending the larval period by delaying metamorphosis does not in most cases lead to disc overgrowth. Interestingly, some evidence suggests that proliferating disc tissue can itself influence the onset of pupariation in Drosophila as well as in other insects (Simpson *et al.* 1980; Bryant and Simpson 1984). However, details of a potential interaction between disc growth and the timing of metamorphosis remain unclear.

Insight into the mechanisms that act in the disc itself to control organ size has come from the identification of mutations that act cell autonomously to cause increased growth of imaginal tissue. These mutations disrupt a subset of Drosophila *t*umor *s*uppressor *g*enes (TSGs) and are generally divided into two categories: "hyperplastic" and "neoplastic" TSGs (Hariharan and Bilder 2006). Mutations in hyperplastic TSGs lead to larger discs with relatively little effect on epithelial structure and, often, differentiation of the tissue. By contrast, mutations in neoplastic TSGs cause imaginal cells to lose epithelial polarity and usually also block terminal differentiation.

A relatively large number of hyperplastic TSGs have been identified, and studies have assigned many of these into several signaling pathways whose mechanisms of action on cell growth, cell death, and cell cycle regulation are becoming increasingly clear. By contrast, only

[1]*Corresponding author:* Department of Molecular and Cell Biology, 142 LSA 3200, University of California, Berkeley, CA 94720-3200. E-mail: bilder@berkeley.edu

seven neoplastic TSGs have been reported to date. Three of these—*scrib*, *dlg*, and *lgl*—encode cytoplasmic proteins with various protein–protein interaction domains (Jacob *et al.* 1987; Woods and Bryant 1991; Bilder and Perrimon 2000). Four others—*avl*, *Rab5*, *tsg101*, and *vps25*—encode components of the endocytic machinery (Lu and Bilder 2005; Moberg *et al.* 2005; Thompson *et al.* 2005; Vaccari and Bilder 2005; Herz *et al.* 2006). The relationship between the cytoplasmic scaffolds and the endocytic regulators, the mechanism of action of these proteins in cell polarity, and in particular how they each act to restrain cell proliferation remains mysterious. Identification of additional neoplastic TSGs in the Drosophila genome may shed light on these mechanisms.

There has not yet been a systematic attempt to isolate neoplastic TSGs. Any such attempt must cope with the significant maternal contribution of known neoplastic TSGs, which prevents detection of mutant phenotypes in zygotically mutant embryos. While the phenotypes of neoplastic TSGs are dramatic in the larval imaginal discs, only *scrib*, *dlg*, and *lgl* have sufficient maternally provided transcript to enable zygotically homozygous animals to survive to L3, when they grow to be distinctively "giant" larvae (Gateff and Schneiderman 1967; Stewart *et al.* 1972; Perrimon 1988; Bilder *et al.* 2000). Instead, *avl*, *Rab5*, *tsg101*, and *vps25* homozygotes die as L1 larvae without obvious phenotypes. The neoplastic phenotypes of these latter genes were detected either in labor-intensive follicle cell screens or in assays dependent on a nonautonomous growth phenotype that is associated with *tsg101* and *vps25* but not shared by other known neoplastic TSGs. These limitations mean that the question of how many genes in Drosophila act to prevent neoplastic growth remains unaddressed.

We have therefore developed a novel and efficient screen for identifying new neoplastic TSGs, based on analysis of genetic mosaic larvae. Strikingly, while eye discs are not themselves required for viability, our data demonstrate that disruption of known neoplastic TSGs in the eye discs alone induces nonautonomous defects that result in death prior to adult eclosion. These defects are associated with delayed or defective pupation and are consistent with a requirement for diminished disc proliferation prior to the onset of metamorphosis. We exploit this pupation-defect phenotype to carry out a genetic mosaic screen for new neoplastic TSGs. Screening of two chromosome arms using this strategy resulted in the identification of at least seven new neoplastic TSGs and illustrates that many unidentified neoplastic TSGs exist in the Drosophila genome.

MATERIALS AND METHODS

Drosophila stocks: EMS screening was conducted using isogenized stocks of *w; FRT40* and *w; FRT82. Gla/CyO TwiGal4 UAS-GFP*, *Lyra/TM6B*, and *TM3 hshid/TM6B* were used to balance and stock mutant chromosomes. The MENE (*m*utant *e*ye disc *n*o *e*closion) screen on 2L and 3R utilized the lines *yw; eyFLP cl GMR-hid FRT40/CyO TwiGal4 UAS-GFP* and *yw;; eyFLP cl GMR-hid FRT82/TM6C*, respectively. In the above stocks, "*cl*" indicates an anonymous mutation that kills cells when homozygous. We employed *CycE FRT40* and *cl R3 FRT82* as stocks carrying additional cell-lethal mutations. Alternative *FLPase* systems tested were *ey3.5FLP; CycE FRT40/CyO*, *ey3.5FLP;; cl R3 FRT82/TM6*, and *UbxFLP; cl FRT40* and *UbxFLP;; cl FRT82. Act5c>CD2>Gal4 UAS-GFP/CyO; hsFLP MKRS/TM6B* was used to assess FLP gene expression and *eyFLP; FRT40 ubGFP/CyO* and *eyFLP; cl ubGFP/CyO* were used to assess mitotic recombination. Other alleles utilized were $tsg101/ept^{2}$, $rab5^{2}$, $vps25^{A3}$, avl^{1}, $scrib^{2}$, lgl^{4}, $warts^{datsX1}$, $warts^{MGH1}$, $mats^{e235}$, $hippo^{40\text{-}47}$, and sav^{3}.

EMS mutagenesis: Male flies carrying an isogenized *FRT* chromosome were starved for 8 hr and subsequently fed a 25-mm EMS solution overnight at room temperature. To screen the 2L chromosome arm, mutagenized *FRT40* males were mated *en masse* to *Gla/CyO TwiGal4 UAS-GFP* females. Single F_1 males of the genotype **FRT40/Cyo TwiGal4 UAS-GFP* were each crossed to three females of the genotype *eyFLP cl GMR-hid FRT40/CyO TwiGal4 UAS-GFP*. Absence of non-*CyO* adults in the F_2 progeny indicated a positive MENE phenotype. Mutant chromosomes were then recovered by crossing F_2 males of the genotype **FRT40/Cyo TwiGal4 UAS-GFP* to *Gla/Cyo TwiGal4 UAS-GFP* females.

To screen the 3R chromosome arm, mutagenized *FRT82* males were mated *en masse* to females of the genotype *Lyra/TM6B*. Single F_1 males of the genotype **FRT82/TM6B* were each crossed to three females of the genotype *eyFLP cl GMR-hid FRT 82/TM6C*. Absence of non-tubby and nonhumeral F_2 adults indicated a positive MENE phenotype. Mutant chromosomes were recovered by crossing F_2 males of the genotype * *FRT82/TM6C* to females of the genotype *TM3 hshid/TM6B*.

Immunohistochemistry and microscopy: All dissections were from wandering third instar larvae taken at the onset of pupariation. Fixations were done at room temperature for 20 min in a methanol-free, 4% paraformaldehyde solution. F-actin stains were done using tetramethylrhodamine isothiocyanate-conjugated phalloidin 1:500 (Sigma, St. Louis). Prior to antibody staining, samples were incubated in a blocking solution of 5% normal goat serum. Primary antibody stains were done at 4° overnight, and secondary antibody stains were done at room temperature for 4 hr. Primary antibodies used were rat anti-Elav 1:50 Developmental Studies Hybridoma Bank (DSHB), rabbit anti-aPKC (Santa Cruz) 1:1000, mouse anti-Dlg (DSHB) 1:100, and mouse anti-Mmp1 1:100 (DSHB) (Zhang *et al.* 2006). Secondary antibodies from Molecular Probes (Eugene, OR) were anti-rat Alexa488, anti-rabbit Alexa488, and anti-mouse Alexa647, all used at 1:200. All images are single confocal sections taken with a TCS microscope (Leica) using ×16/NA 0.5, ×40/NA 1.25, or ×63/NA 1.4 oil lenses. Images were edited with Adobe Photoshop CS and were assembled with Adobe Illustrator 10.

RESULTS

Pupation delay and lethality in animals containing neoplastic TSG mutant eye discs: To identify new neoplastic TSGs, we sought a genetic strategy that would (1) avoid issues of maternal contribution, (2) suit large-scale genetic screening applications, and (3) be sensitive enough to identify all known neoplastic TSGs. The first two criteria are satisfied by genetic mosaic approaches in imaginal discs, specifically in the eye imaginal discs. Eye-disc mosaics can be generated using the

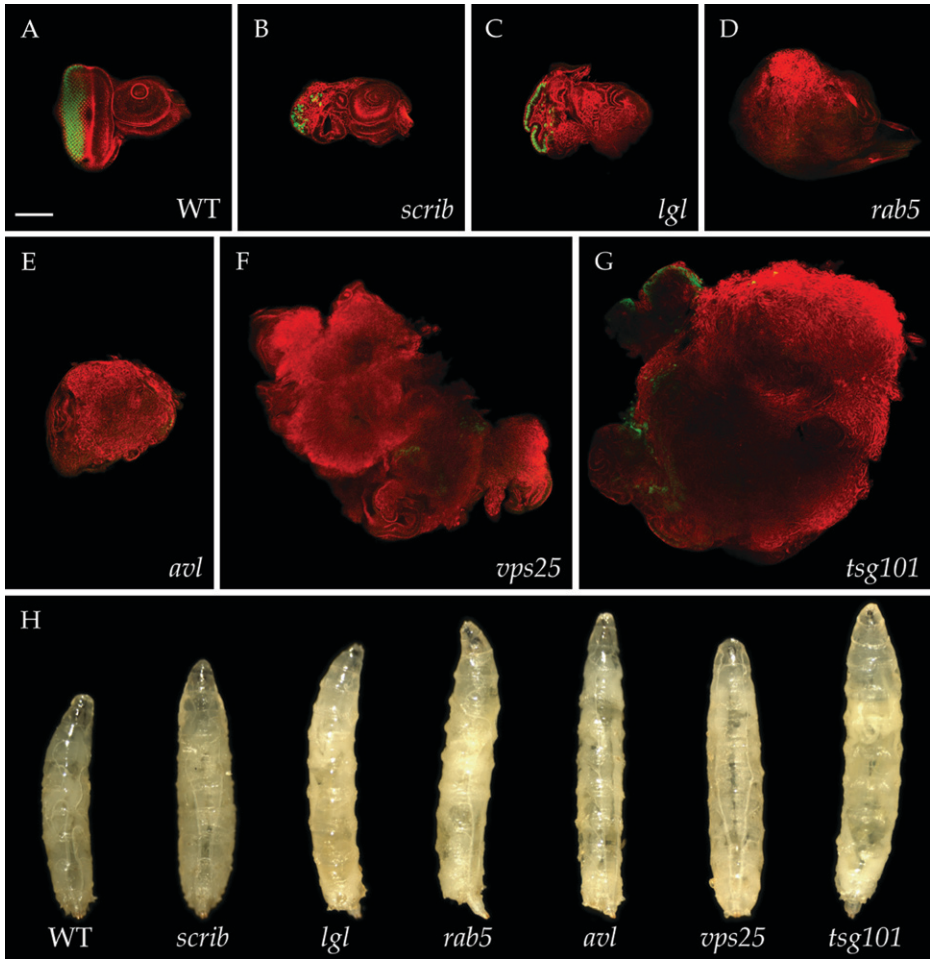

Figure 1.—Phenotypes of neoplastic TSG mutations in the *eyFLP-cell lethal* system. (A–G) Eye imaginal discs stained for cortical actin (phalloidin in red) and neuronal differentiation (Elav in green). Compared to wild type (A), eye discs mutant for six known neoplastic TSGs (B–G) show disorganized cellular architecture and reduced differentiation. Overgrowth of tissue is evident in the cases of *rab5*, *avl*, *vps25*, and *tsg101* (D–G). (H) Phenotypes displayed by mosaic larvae containing neoplastic TSG mutant eye discs, isolated as pupariation commences. Increased larval size is seen in all cases, with *rab5*, *avl*, *vps25*, and *tsg101* (D–G) most obviously giant. Bar, 100 μm.

eyFLP system, in which mitotic recombination is driven in the eye imaginal disc by expression of the FLP recombinase under control of the *eyeless* enhancer (Newsome *et al.* 2000). Such approaches, particularly those that have assessed excess or more rapid growth of mutant tissue in the resultant adult eyes, have successfully identified many of the known hyperplastic TSGs (Hariharan and Bilder 2006). However, as we and others have reported, in imaginal discs mosaic for strong alleles of the neoplastic TSGs *scrib*, *lgl*, *dlg*, *avl*, and *Rab5*, homozygous mutant cells are usually lost due to the process of cell competition (Brumby and Richardson 2003; Pagliarini and Xu 2003; Zeitler *et al.* 2004; Uhlirova *et al.* 2005). *Tsg101* and *vps25* cells survive competition but, like cells mutant for all neoplastic TSGs, fail to differentiate and do not contribute to the adult eye (Moberg *et al.* 2005; Thompson *et al.* 2005; Vaccari and Bilder 2005; Herz *et al.* 2006). Thus, in a genetically mosaic imaginal disc, neoplastic mutant cells do not overgrow to form a tumor that can be easily detected in either larvae or adults.

We therefore adopted an experimental context in which cell competition was eliminated. Such a context can be found using the *eyFLP-cell lethal* system, in which a recessive cell-lethal mutation distal to an FRT recombination site is used to eliminate the genotypically wild-type cells that result as the reciprocal recombination product of homozygous mutant cells (Stowers and Schwarz 1999; Newsome *et al.* 2000). We will refer to these discs, which are predominantly composed of homozygous mutant tissue, as "mutant eye discs" to distinguish them from "mosaic eye discs," in which a significant portion of wild-type tissue remains. We compared the phenotypes of mutant eye discs for null alleles of six of the neoplastic TSGs (*dlg* was not included) to each other and to wild-type eye discs. In neoplastic TSG mutant eye discs, the mutant tissue survives, loses apicobasal polarity, and fails to undergo terminal differentiation (Figure 1, A–G). All of these characteristics are seen in other epithelia mutant for null alleles of neoplastic TSGs, such as the wing imaginal disc and follicle cells, confirming that the use of the *eyFLP-cell lethal* system confers a strong mutant phenotype (Gateff and Schneiderman 1969; Goode and Perrimon 1997; Woods *et al.* 1997; Bilder *et al.* 2000). Interestingly, the amount of overgrowth seen prior to pupariation consistently differed among different genotypes. Eye discs mutant for *tsg101* showed the largest overgrowth, whereas eye discs mutant for three different null alleles of *scrib* were in fact smaller than wild type. Nevertheless, the epithelial disorganization and impaired differentiation was consistent

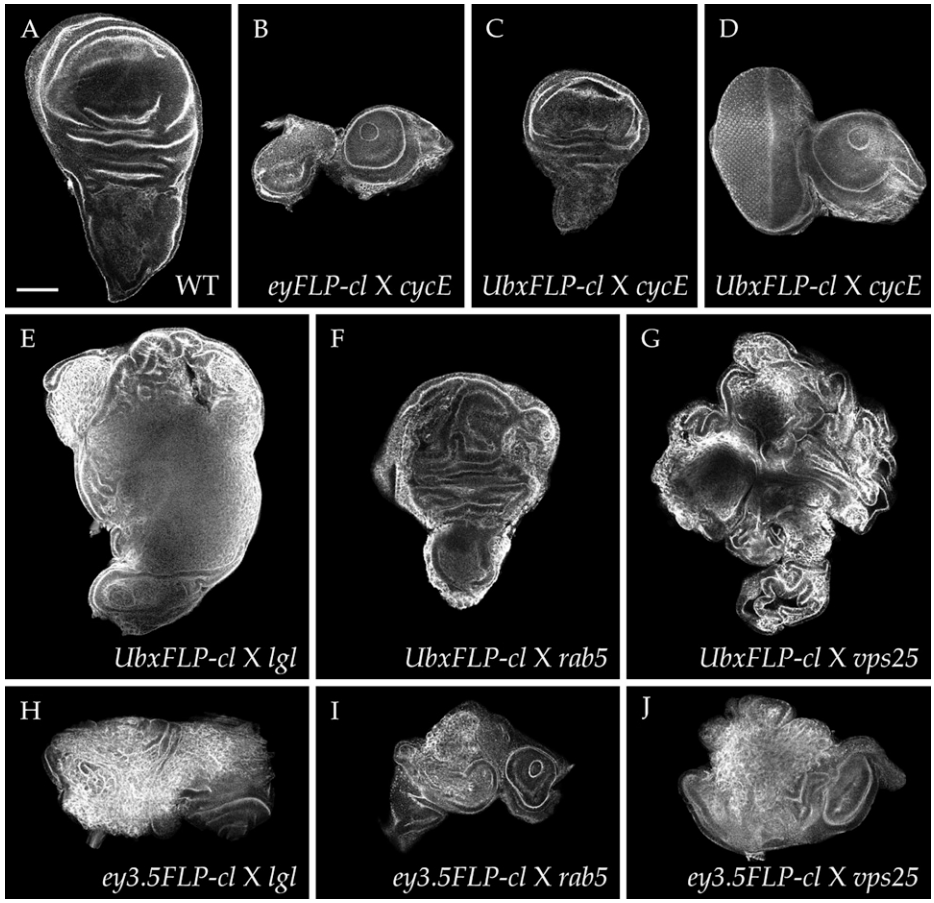

FIGURE 2.—Alternative FLPase systems also cause defects when crossed to neoplastic TSG mutations. (A–D) Degree of recombination in disc tissue, assayed by crossing (B) *eyFLP;cell lethal FRT40* and (C and D) *UbxFLP; cell lethal FRT40* to *cycE FRT40*. Since *cycE* is also a cell-lethal mutation, all recombinant cells in these discs should be eliminated. Recombination driven by *eyFLP* (B) occurs efficiently throughout the disc and results in absence of almost all eye tissue. By contrast, recombination driven by *UbxFLP* (C) is spatially restricted, leaving a large portion of the wing disc intact. The eye disc is unaffected by *UbxFLP* recombination (D). (E–G) Wing disc phenotypes of neoplastic TSG mutations crossed to *UbxFLP-cell lethal*. Neoplastic tissue is largely restricted to the wing pouch in each case. The notum/hinge appears normal, except in *vps25* (G) where nonautonomous hyperplastic overproliferation is seen. All larvae show faulty pupariation (not shown). (H–J) Eye-disc phenotypes of neoplastic TSG mutations crossed to *ey3.5FLP/cell lethal* in pupariation-defective larvae. Disorganization and overgrowth are more mild than that seen with *eyFLP-cell lethal*. All images are phalloidin stained. Bar, 100 μm.

for all of the neoplastic TSG mutations, confirming this as a reliable assay for neoplastic TSG detection.

Surprisingly, we found that larvae generated in this manner and that contained eye discs mutant for each of the neoplastic TSGs failed to develop properly into adults. This contrasts sharply with mutations that eliminate the eye disc, which do not alter larval pupation or adult viability (DICKSON and HAFEN 1993). In the case of *scrib* mutant eye discs, animals died as pharate adults without heads. For the other neoplastic TSG mutations, animals died either as nonpupariating larvae or during pupal stages. Strikingly, mosaic larvae carrying *vps25*, *tsg101*, *avl*, and *rab5* mutant eye discs were distinctly giant in size (Figure 1H). These giant larvae resemble those seen in animals homozygous for *scrib*, *dlg*, and *lgl*, in which the excess growth of discs occurs during an extended larval phase due to a delay in pupation. Animals containing eye discs mutant for the six neoplastic TSGs also display a delay in pupation, which in the strongest case (*vps25*) approached that of homozygous *scrib* animals (data not shown). Importantly, in no case did adults eclose. Therefore, although the generation of giant larvae is a property of only some neoplastic TSG mutant eye discs, pre-eclosion lethality is a fully penetrant phenotype shared by all of those assayed. We named this phenotype MENE (*m*utant *e*ye disc *n*o *e*closion).

The MENE phenotype results from effects on imaginal discs: To test whether the MENE phenotype was specifically induced by neoplastic growth in the eye disc, we employed an alternative FLP recombinase driver that is expressed in other imaginal discs. *UbxFLP* drives recombination in a portion of the wing, haltere, and leg discs at early larval stages, with little recombination evident in eye discs (HUTTERER and KNOBLICH 2005) (supplemental Figure S1G at http://www.genetics.org/supplemental/; data not shown). We built *UbxFLP-cell lethal* stocks and assessed the degree of recombination in wing discs by crossing to chromosomes carrying a distinct set of cell-lethal mutations, reasoning that recombinant tissue homozygous for either cell-lethal mutation would be eliminated. The wing discs in the resultant larvae were partially reduced (Figure 2C) and the overall morphology was retained, indicating that, unlike in the *eyFLP-cell lethal* system (Figure 2B), recombinant cells do not occupy most of the disc and therefore significant wild-type tissue remains. We then crossed *UbxFLP-cell lethal* flies to flies carrying known neoplastic TSG mutations. While eye discs from the resultant larvae were normal (data not shown), wing discs contained regions of neoplastic growth (Figure 2, E–G). Since *UbxFLP*-driven recombination does not occur in the entire wing disc, homozygous mutant cells are still subject to cell competition, and accordingly the disc phenotype was

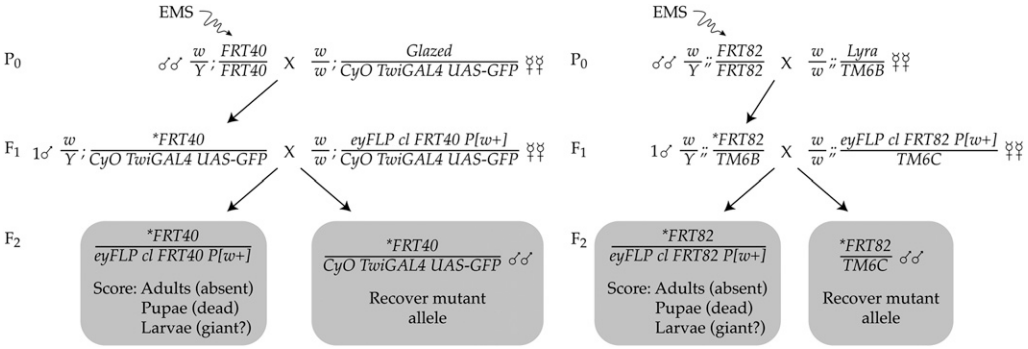

FIGURE 3.—Design of the MENE screen. See text for details.

less extreme than that seen with *eyFLP-cell lethal*. Nevertheless, in all cases no adult eclosers were seen, indicating that recombination of neoplastic TSG mutations driven by *UbxFLP* as well as *eyFLP* can block pupation.

Both the *eyeless* and the *Ubx* promoters drive expression not only in imaginal discs but also in portions of the ring gland (supplemental Figure S1, B and D, at http://www.genetics.org/supplemental/), which secretes hormones that regulate pupation. This observation raised the possibility that recombination in the ring gland rather than imaginal discs induces the MENE phenotype. However, we found that no mitotic recombination was seen in the ring glands of *eyFLP* and *UbxFLP* mosaic larvae when tested with a chromosome carrying a GFP-expressing transgene (Figure S1, F and H), presumably because ring gland FLP expression occurs in postmitotic cells that cannot undergo strand exchange. We also used the *amensiac-GAL4* line (CALDWELL *et al.* 2005) to drive ring gland expression of three constructs that cause neoplastic transformation of disc tissue (an *avl* RNA interference construct, an activated form of atypical protein kinase C, and a truncated version of Crumbs; LU and BILDER 2005) but observed no alterations in pupation or adult viability (data not shown). Finally, we crossed known neoplastic TSG mutations to flies carrying the *ey3.5FLP/cell lethal* system, which utilizes an *eyeless* promoter fragment that is restricted to the eye disc and shows no expression in the ring gland (BAZIGOU *et al.* 2007; supplemental Figure S1, I and J). Although recombination driven by *ey3.5FLP* was variable and often incomplete, larvae that failed to pupate contained eye discs with neoplastic phenotypes resembling those caused by the *eyFLP-cell lethal* system (Figure 2, H–J). We conclude that neoplastic growth in imaginal disc cells themselves leads to defective pupation.

Not all MENE mutants cause overgrowth: Having established that neoplastic TSG mutants can cause the MENE phenotype, we wondered whether other classes of mutations could do so as well. As an initial assessment of this possibility, we analyzed animals containing eye discs mutant for several genes essential for cell viability (see MATERIALS AND METHODS) or that act as hyperplastic TSGs (*pten*, *salvador*). In both cases, adults eclosed, albeit at sub-Mendelian rates, with eyes that were reduced or overgrown, respectively. We therefore anticipated that known hyperplastic TSGs and cell-lethal mutations were unlikely to cause significant background of pre-eclosion lethality in a MENE screen.

We first conducted a pilot screen for MENE phenotypes among a collection of transposon-induced mutations that have been placed on FRT chromosomes (CHEN *et al.* 2005). We crossed 635 of these lines to *eyFLP-cell lethal* stocks and identified 44 lines that displayed the MENE phenotype (supplemental Table S1 at http://www.genetics.org/supplemental/). Among this collection we found alleles of *Rab5* as well as *lgl* that caused neoplastic growth of eye imaginal discs, validating the screen design. Surprisingly, the majority of the other lines showed either wild-type discs or smaller discs, and, unlike *Rab5* and *lgl*, did not prevent eclosion when crossed to *UbxFLP-cell lethal* flies. Inspection of the transposon insertion sites in these lines suggested that a diverse set of genes can be disrupted to cause the MENE phenotype without inducing overgrowth. This pilot screen established that, while loss of growth control is one of multiple pathways that can induce the MENE phenotype, the strategy can indeed be used in a forward genetic screen to detect neoplastic imaginal disc phenotypes.

A genetic screen for pre-eclosion lethality in mosaic larvae: The MENE phenotype, characterized by penetrant pre-eclosion lethality, is seen with all neoplastic TSG mutations in the *eyFLP-cell lethal* system. This finding provided an opportunity to use this easily assayed phenotype as a proxy to identify new neoplastic TSGs. To screen for new mutations that caused the MENE phenotype (Figure 3), we first used EMS to mutagenize male flies that carry an isogenized chromosome with an FRT recombination site near the centromere. These males were mated *en masse* to virgin females carrying a balancer for the mutagenized chromosome; this balancer carried a dominant marker (either *Tubby* or a GFP transgene) such that its presence could be assayed in larval stages. Individual balanced male F_1 progeny of this cross, carrying independent mutations on the FRT chromosome, were then crossed in vials to virgin females of a tester line. The tester carries the *eyFLP* recombinase driver and an autosome with both a

TABLE 1

MENE screen statistics

Chromosome arm	Crosses scored	Mutant chromosomes screened (estimated)	MENE alleles	Initial hit (%)	Class Ib (neoplastic) alleles
2L	16,210	11,347	360	3.2	12
3R	13,709	8,225	543	6.6	24
Total	29,919	19,572	903	4.6	36

Complementation group	No. of alleles
MENE (2L)-A	6
MENE (2L)-B (*lgl*)	5
MENE (2L)-C	2
MENE (3R)-A	4
MENE (3R)-B	3
MENE (3R)-C	2
MENE (3R)-D	2
MENE (3R)-E	2
MENE (3R)-F (*scrib*)	2
MENE (3R)-G (*warts*)	2

matched FRT site and a recessive cell-lethal mutation, all in *trans* to a dominantly marked balancer chromosome. Each vial was ultimately scored for the presence of nonbalanced F_2 progeny. Vials lacking such progeny were considered a "hit" and evaluated, using the markers present on the balancer chromosomes to determine whether nonbalanced pupae, puparia, or larvae were present. Although the animals with mutant eye discs in "hit" vials were dead, the mutant chromosome was recovered in balanced siblings and used to establish a stock.

The MENE screen was carried out on chromosomes 2L (using FRT40) and 3R (using FRT82). Overall, we screened 19,572 mutant chromosomes and isolated 903 individual MENE mutations, yielding a hit rate of 4.6%. The statistics for each arm are given in Table 1.

As a secondary screen, we isolated genetically mosaic larvae from each cross that gave a MENE phenotype and dissected the mutant eye imaginal discs. Phalloidin staining allowed an assay of the size of the disc as well as initial assessments of epithelial organization (the presence of folds with apically enriched actin) and photoreceptor determination (the presence of actin organized into pre-ommatidial clusters). Mutations were provisionally categorized on the basis of this assay into one of five different classes. Mutations that gave discs larger than wild type were considered tumor suppressor mutations (class I). Those that retained epithelial organization were classified as hyperplastic (class Ia), while those with significant portions of tissue where epithelial organization was lost were classified as neoplastic (class Ib). Mutations with consistent phenotypes that did not show tissue-size difference were classified as "other" (class II). Mutations in which disc size was reduced but polarity was unaffected were classified as "small disc" (class III). Other mutations were classified as "no consistent defect" (class IV).

The distribution within the classes was as follows: 55% gave no consistent defect (class IV), 29% showed a small disc phenotype (class III), and 6% gave a consistent phenotype that did not alter disc size (class II), while 6% gave apparent hyperplastic overgrowth (class Ia) and 4% gave apparent neoplastic overgrowth (class Ib). Examples of the class Ia (hyperplastic) mutants are shown in Figure 4, A and B. Phenotypes of the class II mutants included discs that showed general defects in epithelial organization (Figure 4, C and D), severely impaired photoreceptor differentiation (Figure 4, E and F), excess axonal fibers (Figure 4, G and H), and increased actin polymerization (Figure 4, I and J). Examples of the class III (small disc) mutants are shown in Figure 4, K and L. Distinctive phenotypes allowed us to identify three alleles of *capulet* among the elevated actin mutants (Figure 4J) and two alleles of *kuzbanian* among the small disc mutants (Figure 4K). As in the pilot screen, the majority of mutations that give a MENE phenotype do not cause the production of larger imaginal discs, confirming that loss of growth control is only one of multiple pathways that can induce the MENE phenotype.

Neoplastic TSGs among the MENE complementation groups: We focused our final analysis on the new mutations that caused class Ib (neoplastic) disc phenotypes. These mutants formed 10 complementation groups represented by multiple alleles. *MENE (2L)-A* has six alleles, *MENE (2L)-B* has five alleles, *MENE (3R)-A* has four alleles, and *MENE (3R)-B* has three alleles, while *MENE (2L)-C* and *MENE (3R)-C*, *-D*, *-E*, *-F*, and *-G* are represented by two alleles each. The phenotypes of these mutants are shown in Figure 5.

We first assessed the isolation of mutations in known neoplastic TSGs by complementation. These tests revealed that *MENE (2L)-B* is allelic to *lgl* and that *MENE (3R)-F* is allelic to *scrib* (Figure 5, B and I). The *lgl* and *scrib* alleles isolated in the MENE screen all appeared to

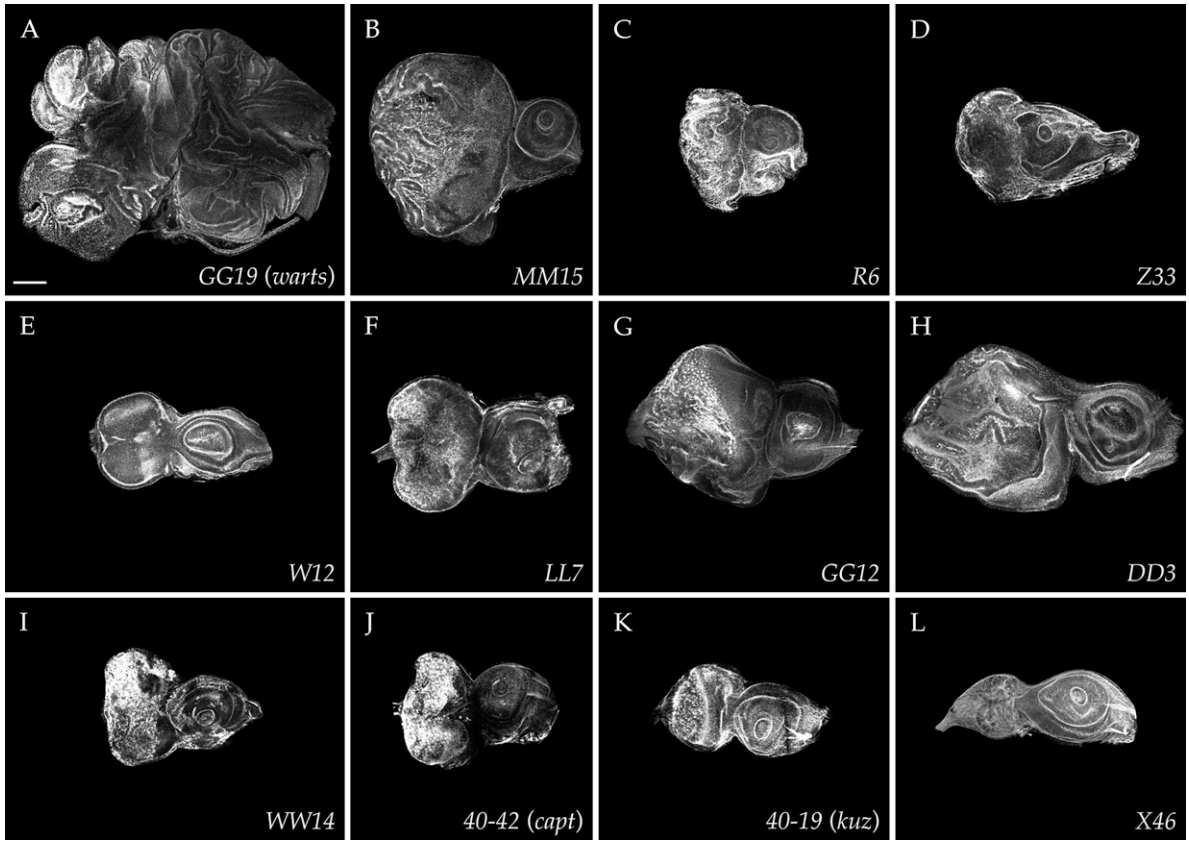

Figure 4.—Examples of eye-disc phenotypes from the MENE screen. Phalloidin stains of MENE allele mutant eye discs reveal phenotypes of hyperplastic growth (A and B), disrupted epithelial organization (C and D), impaired formation of pre-ommatidial clusters (E and F), excess axonal fibers (G and H), increased actin polymerization (I and J), and decreased disc size (K and L). Bar, 100 μm.

be strong, as their phenotype resembled that seen using null alleles (Figure 1). While the isolation of multiple alleles of known neoplastic TSGs served as a positive control validating the success of the screen, we did not identify any alleles of *Rab5*. Therefore, at least on chromosome arm 2L, the MENE screen did not reach saturation.

Initial categorization of MENE mutants in the secondary screen was based on actin staining of imaginal discs, which provides only a general sense of tissue architecture and differentiation. To assess whether the class Ib mutations truly showed neoplastic phenotypes, we examined three characteristics more closely. First, we tested for the presence of Elav immunoreactivity, which reflects differentiation into a neuronal fate and found that Elav was absent in the majority of disc tissue mutant for all eight complementation groups (Figure 6, A–C). Second, we examined the distribution of markers for the polarized apical (atypical protein kinase C) and basolateral (large disc) membrane domains and found that seven of the complementation groups showed an expansion of apical markers that were intermixed with the basolateral domain (Figure 6, F and G). Finally, we asked whether the mutant discs expressed matrix metalloprotease 1 (Mmp1), which is upregulated in tissue mutant for known neoplastic tumor suppressors (Page-McCaw *et al.* 2003; Uhlirova and Bohmann 2006; Beaucher *et al.* 2007; Srivastava *et al.* 2007; our unpublished results), and found upregulation of Mmp1 in tissue mutant for seven of the complementation groups (Figure 6, K and L). Expanded apical domains, loss of terminal differentiation, and upregulation of Mmp1, shown for a *MENE(3R)-A* allele in Figure 6, are all characteristic phenotypes caused by known neoplastic TSG mutations. We therefore conclude that seven of the complementation groups represent *bona fide* neoplastic TSGs that have not been previously identified.

Only one complementation group, *MENE(3R)-G*, formed a phenotypic class separate from the others in the above assays. Despite overgrowth, a failure to differentiate (Figure 6C), and partially disrupted epithelial organization (Figure 6H), tissue mutant for these alleles did not show Mmp1 upregulation (Figure 6M). We found that both *MENE(3R)-G* alleles failed to complement *warts*, a TSG which is removed by a deficiency that fails to complement *MENE(3R)-G* and whose loss has been described as causing altered epithelial architecture (Justice *et al.* 1995; Xu *et al.* 1995). We compared the phenotypes of *MENE(3R)-G* mutant eye discs to those of an X-ray-induced amorphic *warts* allele and an EMS-induced hypomorphic allele isolated in an adult eye screen. We found that, like our *MENE(3R)-G* alleles, disc

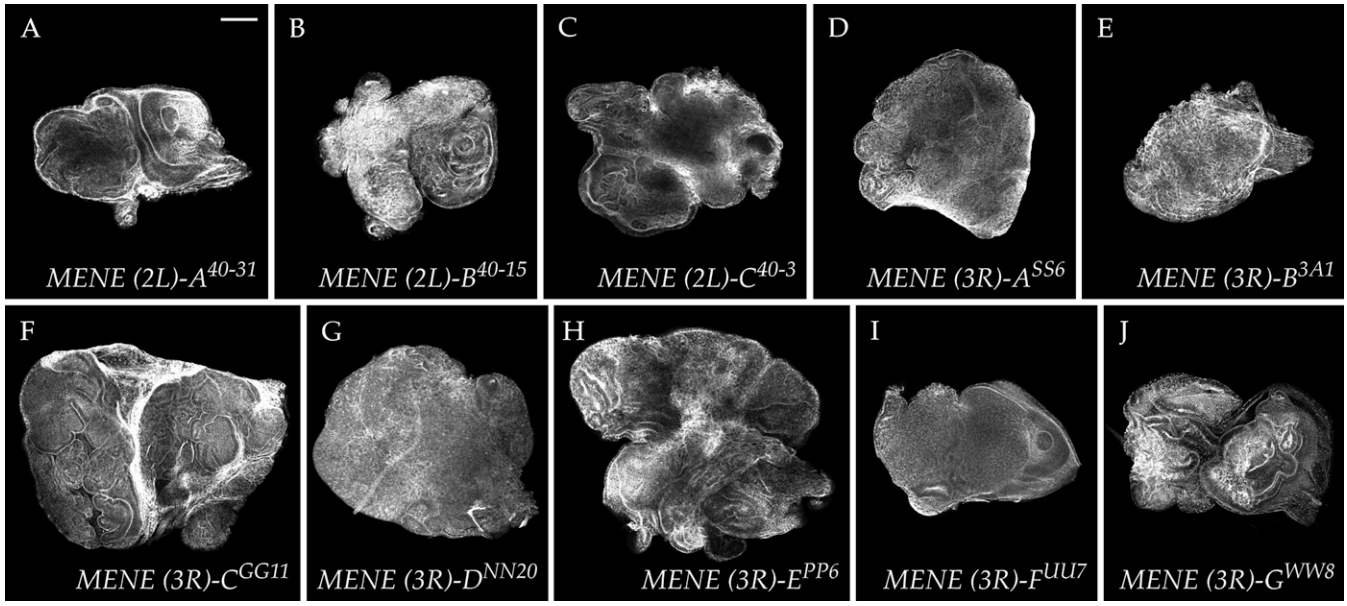

Figure 5.—Neoplastic-like eye-disc phenotypes of MENE mutations. Phalloidin stains of complementation groups that show epithelial disorganization accompanied by upregulated actin polymerization and overgrowth. Overgrowth is mild with *MENE (2L)-A* (A) and *MENE (3R)-B* (E), intermediate with *MENE (2L)-C* (C) and *MENE (3R)-A*, and *-D* (D and G), and most dramatic with *MENE (3R)-C* (F) and *MENE (3R)-E* (H). *MENE (2L)-B* (B) is allelic to *lgl*, *MENE (3R)-F* (I) is allelic to *scrib*, and *MENE (3R)-G* (J) is allelic to *warts*. Bar, 100 μm.

tissue homozygous for the amorphic *warts* allele does not undergo neuronal differentiation and shows disrupted epithelial architecture similar to that described above (Figure 6, D and I). By contrast, hypomorphic *warts* alleles cause strong disc overgrowth but maintain epithelial organization and polarity and show normal photoreceptor differentiation (Figure 6, E and J). While we identified six additional *warts* alleles among the class 1a (hyperplastic) MENE mutations, no alleles of *salvador* or *mats*, two other members of the *warts*-signaling pathway, were found in this collection. We further confirmed that molecularly characterized, strong alleles of *salvador*, *mats*, and *hippo* do not show either the failure of neuronal differentiation or the architectural disruptions of strong *warts* alleles (Figure 6, N and P); furthermore, flies bearing *salvador* and *mats* mutant eyes eclose. These results indicate that *warts* has additional functions beyond those of other members of its signaling pathway, including regulation of differentiation and cell architecture, and suggest that loss of these functions in strong *warts* mutant alleles contributes to their ability to induce the MENE phenotype.

DISCUSSION

The MENE screen and TSG identification: Genetic mosaic screens for TSGs in Drosophila adults have precipitated critical contributions to the understanding of the regulation of organ size. These contributions include the role of insulin signaling and the TOR pathway in promoting cell and tissue growth as well as the definition of a novel growth-regulating pathway involving the Warts kinase (Edgar 2006; Pan 2007). However, the identification of TSGs in screens that rely on detecting growth phenotypes in adult eyes is constrained by several limitations. First, TSG mutant cells must be retained in the eye disc. This is not an issue when cells are faster growing with normal organization, but mutant cells that grow slowly, yet fail to cease proliferation, are usually eliminated by cell competition, while those that have epithelial defects may be extruded from the disc. Second, TSG mutant cells must be capable of terminal differentiation into photoreceptors. Differentiation capacity is not inherently linked to growth control and in fact is often compromised in human tumor cells. Third, the overgrowing TSG mutant larval tissue must not cause lethality of the adult. Accordingly, neoplastic TSG mutations, which cause slow, persistent growth of poorly differentiated, disorganized cells and can interfere with pupation, were not identified in the adult mosaic screens. Interestingly, the MENE screen identified mutations that cause hyperplastic as well as neoplastic growth. Some of the hyperplastic mutations, such as the strong alleles of *warts*, prevent differentiation into neuronal tissue and would thus have been missed in adult-based eye screens. The MENE screen thus acts in a complementary way to adult eye screens and has similar potential for unraveling novel growth-regulatory pathways.

The MENE screen reported here, which covered ~40% of the genome, identified at least seven clear complementation groups that represent new nTSGs. While not saturating, the isolation of multiple alleles of known neoplastic TSGs as well as most new complementation groups suggests that we have identified many of

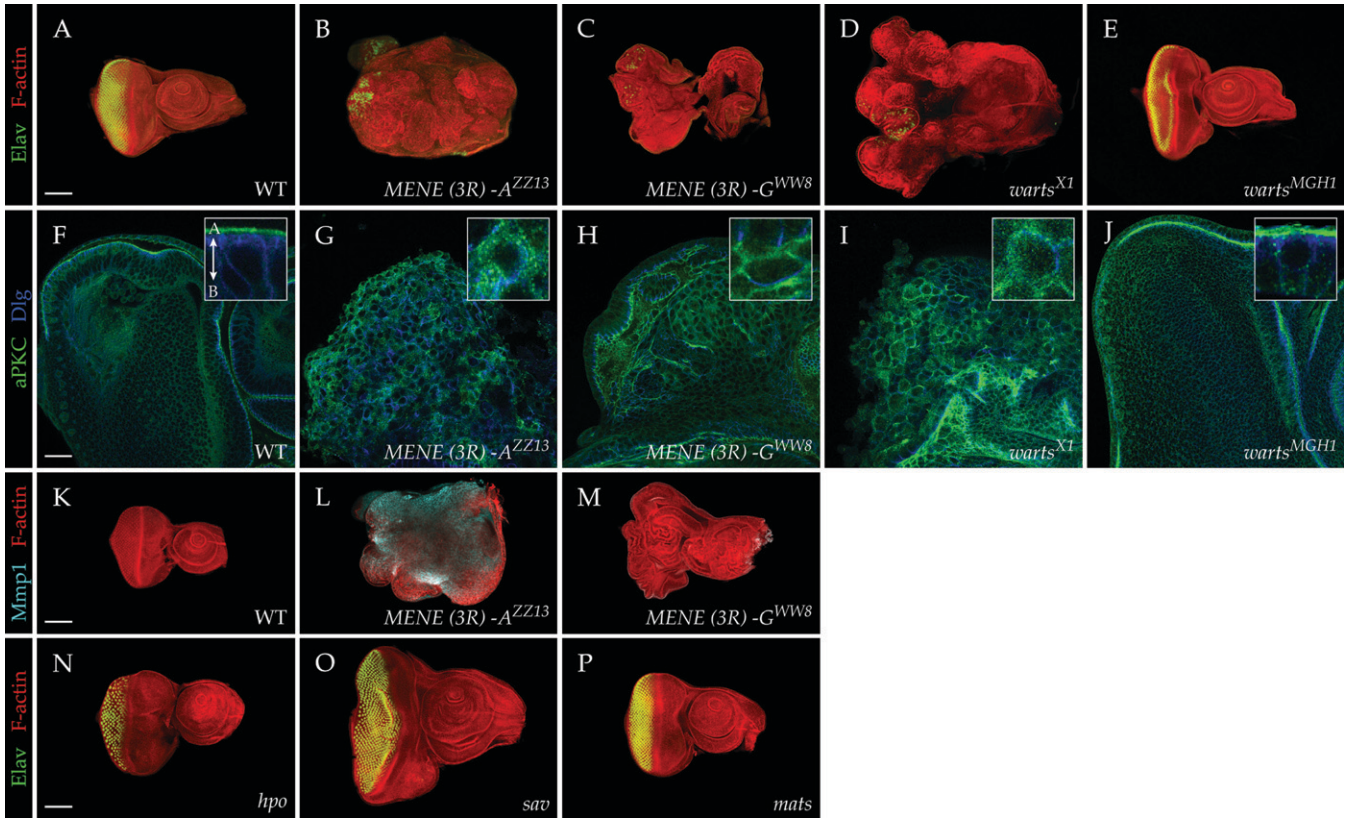

Figure 6.—Epithelial polarity and differentiation defects in MENE mutant eye discs. (A–E) Neuronal differentiation of eye discs shown by staining with antibodies to Elav (green; phalloidin staining is red). Neuronal differentiation is strongly impaired in *MENE(3R)-A ZZ13* (B), the *warts* allele *MENE(3R)-F WW8* (C), and *warts X1* (D) but not *warts MGH1* (E). (F–J) Epithelial polarity of eye discs shown by staining with antibodies to aPKC (green) and Dlg (blue), which are found, respectively, in the apical and lateral regions of wild-type cells (F). High-magnification insets (F–J) show individual cells, with the arrow in the inset in F indicating the apicobasal axis. Eye discs mutant for *MENE(3R)-A* show altered polarity characterized by an expansion of aPKC throughout the plasma membrane (G). *MENE(3R)-F WW8* shows a more limited expansion of apical aPKC (H). Intermediate between the amorphic *warts* allele *X1* (I) and the hypomorphic *warts* allele *MGH1* (J). (K–M) Mmp1 staining (cyan) is elevated in *MENE(3R)-A ZZ13* (L) but not in *MENE(3R)-F WW8* (M). (N–P) Unlike strong *warts* alleles, neuronal differentiation and epithelial organization is not impaired in eye discs mutant for strong *hpo* (N), *sav* (O), or *mats* (P) alleles. Bar in F indicates 25 μm for F–J, and bars in A, K, and N indicate 100 μm for A–E and for K–P.

the genes on 2L and 3R that can mutate to this phenotype. All of the new mutations show an expansion of apical membrane domains in the overgrowing disc tissue, providing further evidence for the close coupling between polarity and proliferation control in Drosophila. The seven complementation groups identified here now double the number of known neoplastic TSG loci, which had previously been identified using various alternative strategies. Notably, lethal-phase analysis indicates that homozygotes for all seven new complementation groups die during early larval stages and would not have been identified in zygotic "giant larvae" screens. Moreover, in preliminary experiments we have been unable to recover follicle clones for *MENE(3R)-A* and *-E*; these alleles at least would have been missed in follicle cell-based screens. Phenotypic and molecular analysis of the mutants is ongoing and will reveal whether the affected genes act through mechanisms similar to the junctional scaffold proteins, the endocytic regulators, or reveal additional pathways that shed light on why normal epithelial structure is required for disc size control.

Imaginal disc proliferation and metamorphosis: In this article, we describe a genetic screening strategy that uses defective pupation as a proxy phenotype to detect mutations that cause imaginal disc overgrowth. Previous work has suggested that the presence of dividing disc cells in an L3 larva can interfere with pupation (Simpson *et al.* 1980). An associated mechanism has not been uncovered but presumably would involve a humoral factor that acts on the neuroendocrine axis to inhibit production of metamorphosis-promoting hormones. In this manner, the autonomous growth control mechanism of the imaginal disc could be coupled to the timing and coordination of metamorphosis throughout the animal. Thus, attainment of proper disc size, as assessed by cessation of most disc cell proliferation, could be used as a "checkpoint" to be cleared before initiating the irreversible process of pupation. In the

MENE screen, we suggest that the presence of excess cell division or continually dividing cells ectopically activates this checkpoint to delay or disrupt the normal process of pupation.

The formation of giant L3 larvae along with delayed or defective pupation is a well-known phenotype of animals homozygous for many TSG mutations, including members of both the neoplastic and the hyperplastic classes (Gateff and Schneiderman 1967; Stewart *et al.* 1972; Tao *et al.* 1999; Bilder *et al.* 2000; Stewart *et al.* 2003; Read *et al.* 2004). In such animals, all tissue is mutant, and overgrowth often occurs in the brain as well as in the eight pairs of imaginal discs. Our results with the *eyFLP-cell lethal* system show that a failure to cease proliferation in the pair of eye discs alone can impair pupation in the entire organism, and in some cases induce a giant larva phenotype resembling that of zygotically homozygous mutant animals. We also observe a correlation between the amount of overgrowing tissue and the stage of defective pupation, in which large overgrowths block pupariation whereas small overgrowths do not visibly alter pupation until pharate stages. These results recall those seen with experiments examining regeneration of imaginal discs in irradiated larvae, where the degree of pupation delay correlates with the amount of regenerating tissue (Simpson *et al.* 1980). Interestingly, those experiments also pointed to a threshold amount of proliferation required to induce pupation delay; that threshold—one pair of discs—is met by our screening strategy. Our results thus support a model in which a signal emanating from proliferating disc cells can repress pupation and cessation of proliferation releases this checkpoint (Simpson *et al.* 1980; Zitnan *et al.* 1993).

Although the MENE screen was effective in isolating genes controlling imaginal disc growth, the majority of MENE mutations did not cause oversized discs. What occurs in these instances to induce pupation defects? While many cases may involve unrelated pathways, it is interesting to speculate that some cases may nevertheless involve cell proliferation. One possibility is that certain mutations that make small discs, or discs with altered epithelial organization, contain both dying as well as continually proliferating cells, and it is the presence of these proliferating cells that activates the pupation checkpoint. An alternative possibility is that certain mutations disrupt communication between growing imaginal discs and the hormonal system that controls metamorphosis. If proliferating disc cells secrete a signal that inhibits pupation, then mutations in negative regulators of such a signal would fail to release this checkpoint. Interestingly, several mutations isolated in the screen produce normal imaginal discs but still block pupation in both the *eyFLP-cell lethal* and *UbxFLP-cell lethal* systems. Further characterization of the MENE mutants may shed light on the mechanisms by which imaginal tissue and the neuroendocrine axis that controls pupation regulate each other.

We thank S. Stowers, F. Roegiers, T. Clandinin, and I. Hariharan for providing fly stocks and A. Halme, I. Hariharan, and the members of the Bilder lab for helpful discussions. This work was supported by grants R01GM068675 (National Institutes of Health) and RSG-07-040-01 (American Cancer Society) to D.B. and an American Heart Association postdoctoral fellowship to T.V.

LITERATURE CITED

Bazigou, E., H. Apitz, J. Johansson, C. E. Loren, E. M. Hirst *et al.*, 2007 Anterograde Jelly belly and Alk receptor tyrosine kinase signaling mediates retinal axon targeting in Drosophila. Cell **128:** 961–975.

Beaucher, M., E. Hersperger, A. Page-McCaw and A. Shearn, 2007 Metastatic ability of Drosophila tumors depends on MMP activity. Dev. Biol. **303:** 625–634.

Bilder, D., and N. Perrimon, 2000 Localization of apical epithelial determinants by the basolateral PDZ protein Scribble. Nature **403:** 676–680.

Bilder, D., M. Li and N. Perrimon, 2000 Cooperative regulation of cell polarity and growth by Drosophila tumor suppressors. Science **289:** 113–116.

Brumby, A. M., and H. E. Richardson, 2003 scribble mutants cooperate with oncogenic Ras or Notch to cause neoplastic overgrowth in Drosophila. EMBO J. **22:** 5769–5779.

Bryant, P. J., and P. Simpson, 1984 Intrinsic and extrinsic control of growth in developing organs. Q. Rev. Biol. **59:** 387–415.

Caldwell, P. E., M. Walkiewicz and M. Stern, 2005 Ras activity in the Drosophila prothoracic gland regulates body size and developmental rate via ecdysone release. Curr. Biol. **15:** 1785–1795.

Chen, J., G. B. Call, E. Beyer, C. Bui, A. Cespedes *et al.*, 2005 Discovery-based science education: functional genomic dissection in Drosophila by undergraduate researchers. PLoS Biol. **3:** e59.

Dickson, B. J., and E. Hafen, 1993 Genetic dissection of eye development in Drosophila, pp. 1327–1362 in *The Development of Drosophila melanogaster*, edited by M. Bate and A. Martinez-Arias. Cold Spring Harbor Laboratory Press, Cold Spring Harbor, NY.

Edgar, B. A., 2006 How flies get their size: genetics meets physiology. Nat. Rev. Genet. **7:** 907–916.

Gateff, E., and H. A. Schneiderman, 1967 Developmental studies of a new mutant of Drosophila melanogaster: lethal malignant brain tumor (l(2)gl 4). Am. Zool. **7:** 760.

Gateff, E., and H. A. Schneiderman, 1969 Neoplasms in mutant and cultured wild-type tissues of Drosophila. Natl. Cancer Inst. Monogr. **31:** 365–397.

Goode, S., and N. Perrimon, 1997 Inhibition of patterned cell shape change and cell invasion by Discs large during Drosophila oogenesis. Genes Dev. **11:** 2532–2544.

Hariharan, I. K., and D. Bilder, 2006 Regulation of imaginal disc growth by tumor-suppressor genes in Drosophila. Annu. Rev. Genet. **40:** 335–361.

Herz, H. M., Z. Chen, H. Scherr, M. Lackey, C. Bolduc *et al.*, 2006 vps25 mosaics display non-autonomous cell survival and overgrowth, and autonomous apoptosis. Development **133:** 1871–1880.

Hutterer, A., and J. A. Knoblich, 2005 Numb and alpha-Adaptin regulate Sanpodo endocytosis to specify cell fate in Drosophila external sensory organs. EMBO Rep. **6:** 836–842.

Jacob, L., M. Opper, B. Metzroth, B. Phannavong and B. M. Mechler, 1987 Structure of the l(2)gl gene of Drosophila and delimitation of its tumor suppressor domain. Cell **50:** 215–225.

Justice, R. W., O. Zilian, D. F. Woods, M. Noll and P. J. Bryant, 1995 The Drosophila tumor suppressor gene warts encodes a homolog of human myotonic dystrophy kinase and is required for the control of cell shape and proliferation. Genes Dev. **9:** 534–546.

Lu, H., and D. Bilder, 2005 Endocytic control of polarity and proliferation in Drosophila. Nat. Cell Biol. **7:** 1232–1239.

Moberg, K. H., S. Schelble, S. K. Burdick and I. K. Hariharan, 2005 Mutations in erupted, the Drosophila ortholog of mammalian tumor susceptibility gene 101, elicit non-cell-autonomous overgrowth. Dev. Cell **9:** 699–710.

Newsome, T. P., B. Asling and B. J. Dickson, 2000 Analysis of Drosophila photoreceptor axon guidance in eye-specific mosaics. Development **127:** 851–860.

Page-McCaw, A., J. Serano, J. M. Sante and G. M. Rubin, 2003 Drosophila matrix metalloproteinases are required for tissue remodeling, but not embryonic development. Dev. Cell **4:** 95–106.

Pagliarini, R. A., and T. Xu, 2003 A genetic screen in Drosophila for metastatic behavior. Science **302:** 1227–1231.

Pan, D., 2007 Hippo signaling in organ size control. Genes Dev. **21:** 886–897.

Perrimon, N., 1988 The maternal effect of lethal(1)discs-large-1: a recessive oncogene of Drosophila melanogaster. Dev. Biol. **127:** 392–407.

Read, R. D., E. A. Bach and R. L. Cagan, 2004 Drosophila C-terminal Src kinase negatively regulates organ growth and cell proliferation through inhibition of the Src, Jun N-terminal kinase, and STAT pathways. Mol. Cell. Biol. **24:** 6676–6689.

Simpson, P., P. Berreur and J. Berreur-Bonnenfant, 1980 The initiation of pupariation in Drosophila: dependence on growth of the imaginal discs. J. Embryol. Exp. Morphol. **57:** 155–165.

Srivastava, A., J. C. Pastor-Pareja, T. Igaki, R. Pagliarini and T. Xu, 2007 Basement membrane remodeling is essential for Drosophila disc eversion and tumor invasion. Proc. Natl. Acad. Sci. USA **104:** 2721–2726.

Stewart, M., C. Murphy and J. W. Fristrom, 1972 The recovery and preliminary characterization of X chromosome mutants affecting imaginal discs of Drosophila melanogaster. Dev. Biol. **27:** 71–83.

Stewart, R. A., D. M. Li, H. Huang and T. Xu, 2003 A genetic screen for modifiers of the lats tumor suppressor gene identifies C-terminal Src kinase as a regulator of cell proliferation in Drosophila. Oncogene **22:** 6436–6444.

Stowers, R. S., and T. L. Schwarz, 1999 A genetic method for generating Drosophila eyes composed exclusively of mitotic clones of a single genotype. Genetics **152:** 1631–1639.

Tao, W., S. Zhang, G. S. Turenchalk, R. A. Stewart, M. A. St. John *et al.*, 1999 Human homologue of the Drosophila melanogaster lats tumour suppressor modulates CDC2 activity. Nat. Genet. **21:** 177–181.

Thompson, B. J., J. Mathieu, H. H. Sung, E. Loeser, P. Rorth *et al.*, 2005 Tumor suppressor properties of the ESCRT-II complex component Vps25 in Drosophila. Dev. Cell **9:** 711–720.

Uhlirova, M., and D. Bohmann, 2006 JNK- and Fos-regulated Mmp1 expression cooperates with Ras to induce invasive tumors in Drosophila. EMBO J. **25:** 5294–5304.

Uhlirova, M., H. Jasper and D. Bohmann, 2005 Non-cell-autonomous induction of tissue overgrowth by JNK/Ras cooperation in a Drosophila tumor model. Proc. Natl. Acad. Sci. USA **102:** 13123–13128.

Vaccari, T., and D. Bilder, 2005 The Drosophila tumor suppressor vps25 prevents nonautonomous overproliferation by regulating notch trafficking. Dev. Cell **9:** 687–698.

Woods, D. F., and P. J. Bryant, 1991 The discs-large tumor suppressor gene of Drosophila encodes a guanylate kinase homolog localized at septate junctions. Cell **66:** 451–464.

Woods, D. F., J. W. Wu and P. J. Bryant, 1997 Localization of proteins to the apico-lateral junctions of Drosophila epithelia. Dev. Genet. **20:** 111–118.

Xu, T., W. Wang, S. Zhang, R. A. Stewart and W. Yu, 1995 Identifying tumor suppressors in genetic mosaics: the Drosophila lats gene encodes a putative protein kinase. Development **121:** 1053–1063.

Zeitler, J., C. P. Hsu, H. Dionne and D. Bilder, 2004 Domains controlling cell polarity and proliferation in the Drosophila tumor suppressor Scribble. J. Cell Biol. **167:** 1137–1146.

Zhang, S., G. M. Dailey, E. Kwan, B. M. Glasheen, G. E. Sroga *et al.*, 2006 An MMP liberates the Ninjurin A ectodomain to signal a loss of cell adhesion. Genes Dev. **20:** 1899–1910.

Zitnan, D., F. Sehnal and P. J. Bryant, 1993 Neurons producing specific neuropeptides in the central nervous system of normal and pupariation-delayed Drosophila. Dev. Biol. **156:** 117–135.

Communicating editor: T. C. Kaufman